Original Article
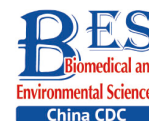
Ezrin Promotes the Proliferation, Migration, and Invasion of Ovarian Cancer Cells*

LI Mo Juan[1,&], XIONG Dan[2,&], HUANG Hao[1,#], and WEN Zhong Yong[1,#]

1. Department of Obstetrics and Gynecology, Nanhai Hospital Affiliated to Southern Medical University, Foshan 528200, Guangdong, China; 2. Department of Hematology, Shunde Hospital of Southern Medical University (The First People's Hospital of Shunde), Foshan 528308, Guangdong, China

Abstract

Objective   The underlying mechanism of Ezrin in ovarian cancer (OVCA) is far from being understood. Therefore, this study aimed to assess the role of Ezrin in OVCA cells (SKOV3 and CaOV3) and investigate the associated molecular mechanisms.

Methods   We performed Western blotting, reverse transcription-quantitative polymerase chain reaction, MTT, cell colony, cell wound healing, transwell migration and invasion, RhoA and Rac active pull down assays, and confocal immunofluorescence experiments to evaluate the functions and molecular mechanisms of Ezrin overexpression or knockdown in the proliferation and metastasis of OVCA cells.

Results   The ectopic expression of Ezrin significantly increased cell proliferation, invasiveness, and epithelial–mesenchymal transition (EMT) in OVCA cells. By contrast, the knockdown of endogenous Ezrin prevented OVCA cell proliferation, invasiveness, and EMT. Lastly, we observed that Ezrin can positively regulate the active forms of RhoA rather than Rac-1 in OVCA cells, thereby promoting robust stress fiber formation.

Conclusion   Our results indicated that Ezrin regulates OVCA cell proliferation and invasiveness by modulating EMT and induces actin stress fiber formation by regulating Rho-GTPase activity, which provides novel insights into the treatment of the OVCA.

Key words: Epithelial ovarian cancer; Ezrin; Proliferation; Invasiveness; RhoA; Stress fiber

INTRODUCTION

Ovarian cancer (OVCA) is the most lethal female gynecological cancer. Most patients with OVCA are diagnosed at an advanced stage due to the lack of early symptoms and available diagnostic techniques. At present, surgery is the main treatment, and platinum and taxane are used for auxiliary chemical system treatment. Unfortunately, more than 80% of OVCA patients develop a recurrent disease after the primary curative surgical approach followed by chemotherapy[1-5]. The median survival time of OVCA patients is short, and the 10-year rates of disease-free survival among patients with recurrent disease are less than 15%[6]. Majority of patients with

recurrent OVCA need additional treatment options. Despite being studied for two decades, the pathobiology of epithelial OVCA has yet to be fully understood due to numerous factors, including the poor understanding of the mechanisms of precursors and tumor progression and the usually late-stage occurrence of this aggressive disease[7,8]. Numerous researchers aim to determine the molecular mechanism that regulates the proliferation and metastasis of OVCA cells.

Ezrin, a member of the ezrin–radixin–moesin (ERM) family, is not only a key membrane cytoskeletal crosslinker, but also involved in signal transduction[9]. High ezrin expression and aberrant localization are observed in clinical cervical cancer specimens; such observation might be an independent effective prognostic marker for evaluating cervical lesions with a high risk of progression to cervical cancer[10,11]. Ezrin has high expression levels in glioblastoma multiforme cells and can enhance cell growth by regulating the activity of Rac1[12,13]. Chen et al.[14] reported that ezrin is overexpressed in OVCA tissues and cells, with the highest expression level in metastatic tissues and cells. Song et al.[15] demonstrated that estrogen-induced ezrin overexpression plays an important role in OVCA metastasis. Thus, we hypothesized that the high expression of ezrin can regulate the growth and metastasis of OVCA cells.

Here, we performed MTT, cell colony, cell wound healing, transwell migration and invasion, RhoA and Rac active pull down assays, and confocal immunofluorescence experiments in the SKOV3 and CaOV3 cell lines to evaluate the functions of ezrin and explore the involved mechanisms.

MATERIALS AND METHODS

Antibodies and Reagents

Ezrin, E-cadherin, and Vimentin monoclonal antibodies and GAPDH polyclonal antibody were all purchased from Santa Cruz Biotechnology Inc. (Dallas, TX, USA). The secondary antibody conjugated to Alexa Fluor 488 or Alexa Fluor 594 was from Beyotime Institute of Biotechnology (Shanghai, China). Peroxidase-coupled secondary antibodies were purchased from Jackson Immunology Research Laboratory (West Grove, Pennsylvania, USA). A RhoA/Rac1/Cdc42 activation assay combo kit (STA-405) was obtained from Cell Biolabs, Inc. (San Diego, CA, USA). The pCMV-FLAG-ezrin plasmids were constructed in our laboratory.

Cell Culture and Treatment

Human ovarian carcinoma cells SKOV3 and CaOV3 were purchased from Cell Resource Center, Institute of Life Science Chinese Academy of Sciences (Shanghai, China). All cell lines were cultured in high-glucose Dulbecco's modified Eagle's medium (DMEM) supplemented with 10% fetal bovine serum (FBS, GE Healthcare, Chicago, IL, USA) and maintained at 37 °C in a humidified atmosphere containing 5% CO_2.

Ezrin siRNA Transfection

SKOV3 and CaOV3 cells were transfected with 100 nmol/L Ezrin siRNA or negative control siRNA using Lipofectamine 2000 (Invitrogen, Carlsbad, CA, USA) in accordance with the manufacturer's instructions. For an effective Ezrin knockdown, a mixture of four siRNAs with a final concentration of 100 nmol/L was used. The mixture included the following sequences: ezrin-siRNA-1: 5'-GCUCAAAGAUAAUGCUAUGTT-3' (forward) and 5'-CAU AGCAUUAUCUUUGAGCTT-3' (reverse), ezrin-siRNA-2: 5'-GGAAUCAACUAUUUCGAGATT-3' (forward) and 5'-UCUCGAAAUAGUUGAUUCCTT-3' (reverse), ezrin-siRNA-3: 5'-GCGCAAGGAGGAUGAAGUUTT-3' (reverse) and 5'-AACUUCAUCCUCCUUGCGCTT-3' (reverse), ezrin-siRNA-4: 5'-GCGCGGAGCUGUCUA-GUGATT-3' (forward) and 5'-UCACUAGACAGCUCCGCG-CTT-3' (reverse). All of the siRNAs were synthesized by Shanghai GenePharma Co., Ltd. (Shanghai, China).

Detection of Protein Expression via Western Blot Analysis

Subconfluent cell cultures were washed twice with cold PBS and then lysed with a lysis buffer [20 mmol/L Tris (pH 7.5), 150 mmol/L NaCl, sodium pyrophosphate, β-glycerophosphate, EDTA, 1% Triton X-100, Na_3VO_4, leupeptin, and 1% protease inhibitor cocktail (Roche Applied Science, Penzberg, Germany)] for 20 min on ice. Cell lysates were centrifuged, and the supernatants were collected. An aliquot of combined extract was used for protein determination using a BCA kit (Thermo Fisher Scientific, Waltham, MA, USA). A total of 50 μg of protein were separated by 10% or 12% SDS-PAGE and transferred to polyvinylidene difluoride membranes (EMD Millipore, Billerica, MA, USA). After blocking in 5% dry skimmed milk for 60 min at room temperature (RT), membranes were incubated with the primary antibodies (dilution, 1 : 2,000) overnight at 4 °C. Next, the membranes were washed with TBST buffer and incubated with horseradish peroxidase-conjugated secondary

antibodies (dilution, 1 : 5,000; ProteinTech Group, Wuhan, China) for 60 min at RT. All antibodies used in the present study were diluted in 5% dry skimmed milk in TBST buffer. An enhanced chemiluminescence kit (Beyotime Institute of Biotechnology, Shanghai, China) was used to detect protein expression. The Western blotting bands were quantified using ImageJ software (version number, 1.42; National Institutes of Health, Bethesda, MD, USA).

MTT Assay

SKOV3 and CaOV3 cells transfected with siRNAs or recombinant plasmids in accordance with the experimental requirements were plated at 96-well plates at a density of 5×10^3 cells in 200 μL DMEM medium with 10% FBS at 37 °C with 5% CO_2. The MTT reagent (Sangon, Shanghai, China) was added to each well at the indicated time points and incubated for 4 h in the CO_2 incubator. The generated formazan was dissolved in 150 μL of DMSO, and the optical density was read at 570 nm on a microplate spectrophotometer. Quintuplicate wells were measured in each treatment group.

Colony Formation Assay

SKOV3 and CaOV3 cells transfected with siRNAs or recombinant plasmids in accordance with the experimental requirements were seeded in 6-well plates at a density of 400 or 200 cells/well. After incubation for 14 d, cells were washed twice with PBS, fixed with methanol, and stained with crystal violet before being counted.

Cell Migration Assay

Transwell chambers with 8 mm membranes (Costar®, Corning, NY, USA) that were placed in 24-well plates were incubated with serum-free DMEM medium at 37 °C for 1 h. Then, 5×10^4 transfected cells in 200 μL serum-free medium were seeded in the upper compartment of the transwell chambers. After incubation for 12 h at 37 °C, the migrating cells that were attached to the lower membranes were stained with crystal violet and counted.

Wound Healing Assay

SKOV3 and CaOV3 cells were transfected with either pCMV-FLAG-vector or pCMV-FLAG-ezrin recombinant plasmids and then seeded onto 6-well plates. After 16 h, the adhered cell monolayers were scratched with a 200 μL pipette tip and incubated in FBS-free medium for 24 h. Wound healing capacity was monitored *via* microscopy at 0, 12, 18, and 24 h.

Cell Invasion Assay

SKOV3 and CaOV3 cells (5×10^4) transfected with siRNAs or recombinant plasmids in accordance with the experimental requirements were resuspended in 200 μL of medium without FBS and then seeded into the top chamber with Matrigel-coated membrane. Subsequently, 500 μL of DMEM medium containing 10% FBS was added to the bottom chamber as a chemical attractant. After incubation for 12 h, the cells were fixed and stained with crystal violet. The invaded cells in five randomly chosen fields of each well were counted.

Reverse Transcription-quantitative Polymerase Chain Reaction (RT-qPCR)

Total RNA was extracted from cultured cells using TRIzol reagent (Thermo Fisher Scientific, Inc.), and DNA was removed using the recombinant DNaseI. cDNA was prepared from 1 μg of total RNA using reverse transcriptase and an iScriptTM cDNA synthesis kit (Bio-Rad Laboratories, Inc., Hercules, CA, USA) in accordance with the manufacturer's protocol. All PCR reactions were performed using SsoFastTM Eva Green Supermix (Bio-Rad Laboratories, Inc.) with the following 39 thermal cycles: 95 °C for 15 s, 60 °C for 15 s, and 72 °C for 20 s. The following primers were used for PCR: Vimentin forward, 5'-CCACCAGGTCCGTGTCCTCGT-3' and reverse, 5'-CGCTGCCCAGGCTGTAGGTG-3'; E-cadherin forward, 5'-TTGCACCGGTCGACAAAGGAC-3' and reverse, 5'-TGGAGTCCCAGGCGTAGACCAA-3'; and GAPDH (control) forward, 5'-AACGGATTT-GGTCGTATTG-3' and reverse, 5'-GGAAGATGGTGAT-GGGATT-3'. The relative concentration of HDAC6 mRNA was calculated using the $2^{-\Delta\Delta Cq}$ method.

RhoA and Rac Active Pull Down Assays

RhoA and Rac1 pulldown activation assays were conducted in accordance with the manufacturer's protocols (STA- 405, Cell Biolabs).

Immunofluorescent Analysis

SKOV3 and CaOV3 cells were grown on polylysine-precoated slides. Cells were fixed with 4% paraformaldehyde for 30 min, permeated with 0.1% Triton X-100 for 10 min at RT, blocked in 10% normal goat serum for 1 h, and then incubated with the primary antibody at 4 °C overnight. After washing, cells were incubated with Alexa Fluor 488-conjugated secondary antibody, followed by nuclear counterstaining with DAPI for 10 min. F-actin was stained with 0.7 μmol/L rhodamine-phalloidin

for 30 min (Invitrogen). Slides were imaged using a 40 × NA 0.75 Oil Dic objective on an inverted laser-scanning confocal microscope (LSM700; Zeiss GmbH, Jena, Germany), and images were captured using Zeiss software.

Statistical Analysis

All statistical analyses were performed using GraphPad Prism 6 software (GraphPad Software, Inc., La Jolla, CA, USA). The significant differences between the two groups were analyzed via two-tailed unpaired Student's t-tests. Data were expressed as the mean ± standard deviation, $n ≥ 3$, unless otherwise stated. $P < 0.05$ indicated a statistically significant difference.

RESULTS

Ezrin Promotes the Proliferation of Epithelial OVCA Cells

To characterize the role of Ezrin in OVCA cells, we examined the expression level of ezrin in human ovarian epithelial cell lines IOSE80 and human OVCA cell lines CaOV3 and SKOV3. The results showed that Ezrin was overexpressed in either CaOV3 or SKOV3 compared with IOSE80 cells, hinting on a correlation between the expression of ezrin and its involvement in the carcinogenesis of OVCA (Figure 1A). To explore the influence of changes in ezrin expression on the proliferation of epithelial OVCA cells, we down- or upregulated ezrin in OVCA SKOV3 and CaOV3 cell lines *via* transfection with siRNA or the FLAG-ezrin over-expression plasmid or their corresponding controls. Transfection with the FLAG-ezrin over-expression plasmid or siRNA significantly up- or downregulated the expression of ezrin in SKOV3 and CaOV3 cells, respectively (Figure 1B). Cell proliferation was detected *via* MTT assay, and data showed that after the suppression of ezrin in SKOV3 and CaOV3 cells, cell proliferation significantly decreased. However, cell proliferation was significantly increased after the upregulation of ezrin in SKOV3 and CaOV3 cells (Figure 1C). The same results were obtained via the colony-formation assay (Figure 1D).

Ezrin Promotes the Migratory and Invasive Ability of Epithelial OVCA Cells

To corroborate the role of ezrin in mediating cell migration, we used a modified Boyden chamber migration assay and wound healing methods to assess whether the ezrin expression changes in SKOV3 and CaOV3 OVCA cells could affect cell motility. As shown in Figure 2, SKOV3 and CaOV3 cells with an increased level of ezrin had significantly higher migratory ability compared with the control group, whereas significantly less cell migration was detected in SKOV3 and CaOV3 cells subjected to siEzrin transfection for 24 h. The same results were obtained via the wound healing assays, indicating that ezrin positively regulates the migration ability of OVCA cells (Figure 2 and Supplementary Figure S1 available in www.besjournal.com).

We then investigated whether ezrin could influence the invasive capacity of OVCA cells, which are a key metastatic phenotype. Transwell invasion assays were used to assess the invasion of SKOV3 and CaOV3 cells transfected with pCMV-FLAG-ezrin, which showed significantly stronger Matrigel invasion capacity compared with the control group. Reciprocally, when SKOV3 and CaOV3 cells were transfected with siEzrin, the invasiveness of the matrix gel decreased in comparison with the control group transfected with siNC (Figure 3A and 3B). This result indicates that ezrin enhances the invasiveness of epithelial OVCA cells.

Ezrin Upregulates Vimentin and Downregulates E-cadherin Expression to Promote Epithelial–mesenchymal Transition

Epithelial–mesenchymal transition (EMT) refers to the process in which polar epithelial cells lose their polarity and cell–cell adhesion ability, rearrange the cytoskeleton, and gain the ability of migration and invasion. This process is involved in various physiological and pathological processes that regulate embryonic development and tissue repair and is also associated with the occurrence and development of fibrous diseases and cancer. Vimentin is used as a marker of mesenchymally derived cells or cells undergoing EMT. E-cadherin, which is also a hallmark of EMT, is expressed in most normal epithelial tissues[16].

We then investigated the effects of ezrin on EMT. Compared with cells transfected with control plasmids, SKOV3 and CaOV3 cells transfected with FLAG-ezrin expressing plasmids showed upregulated vimentin, whereas the expression of epithelial marker E-cadherin was downregulated. By contrast, the protein levels of E-cadherin were upregulated, and the protein levels of vimentin were downregulated in SKOV3 and CaOV3 cells transfected with anti-ezrin siRNA compared with cells transfected with siNC (Figure 4A). RT-qPCR assays were also used to detect these EMT markers

(vimentin and E-cadherin) in SKOV3 and CaOV3 cells with transfection of anti-ezrin siRNA or FLAG-ezrin expressing plasmids or their corresponding controls.

Ezrin overexpression increased the mRNA expression of vimentin and decreased the mRNA expression levels of E-cadherin in SKOV3 and CaOV3 cells. Ezrin
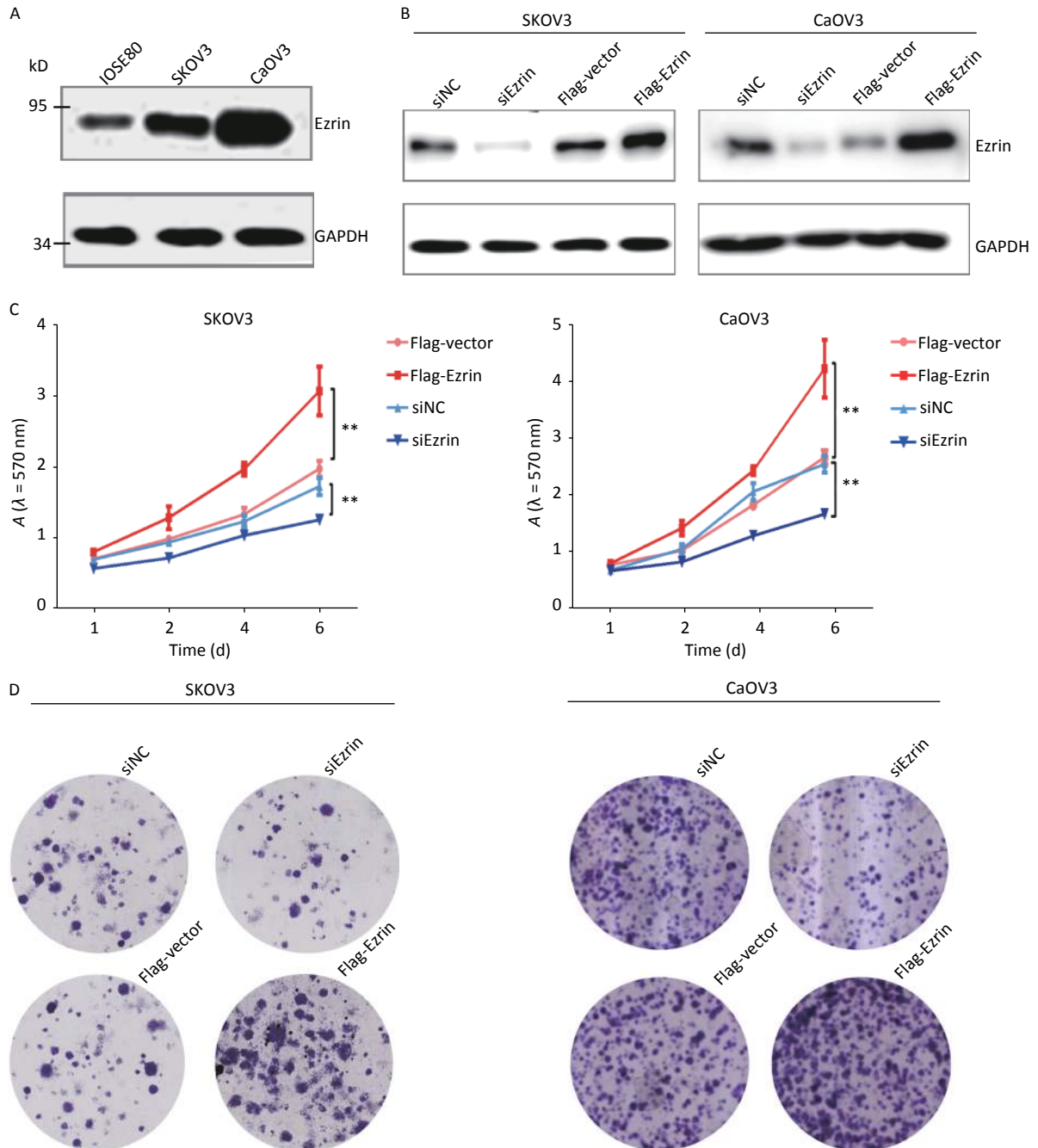

Figure 1. Effects of ezrin on cell proliferation in ovarian carcinoma cells. (A) The protein levels of ezrin were analyzed *via* Western blot analysis in IOSE80, CaOV3, and SKOV3 cells. (B) SKOV3 and CaOV3 cells were transfected with siEzrin or FLAG-ezrin and their respective negative controls for 24 h. The efficiency of the knockdown or upregulation of ezrin was verified *via* Western blot analysis. (C) Cell growth was determined *via* MTT assay after ezrin overexpression or knockdown in SKOV3 and CaOV3 cells. Data are presented as mean ± standard deviation, $n \geq 3$, [**]$P < 0.01$. (D) Colony formation assays were performed on the upregulation and downregulation of ezrin in SKOV3 and CaOV3 cells.

knockdown decreased the mRNA expression of vimentin and increased the mRNA expression levels of E-cadherin in SKOV3 and CaOV3 cells (Figure 4B–C). These results are similar to the above Western blot results, suggesting that ezrin induces

EMT in epithelial OVCA cells.

Ezrin Mediates Cytoskeletal Rearrangement by Regulating RhoA Activity

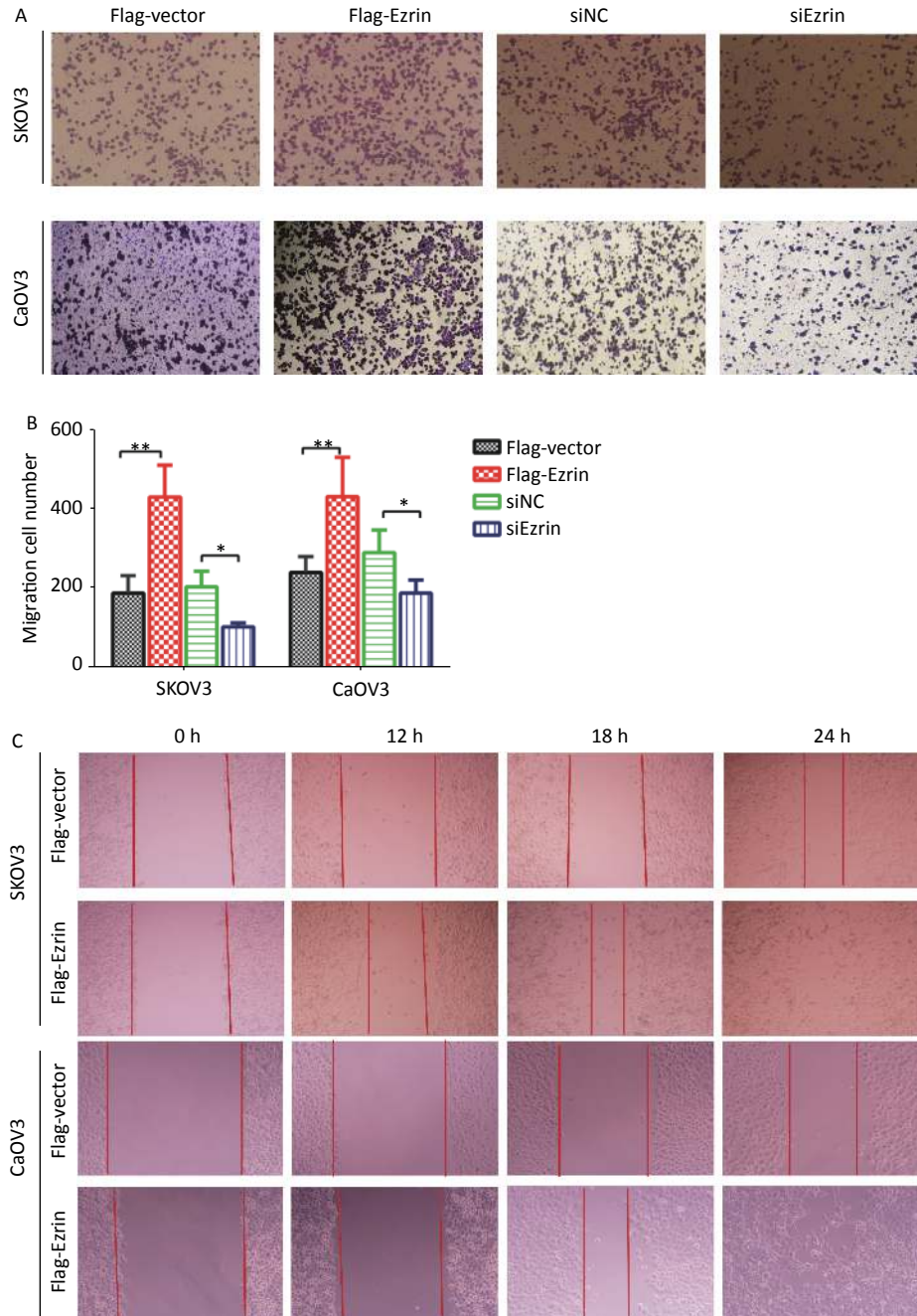ERM proteins can reciprocally regulate the small

Figure 2. Effects of ezrin on cell migration in ovarian carcinoma cells. (A) Cell migration assays were performed on the upregulation and downregulation of ezrin in SKOV3 and CaOV3 cells. (B) Statistical results of cell migration efficiency. Data are presented as mean ± standard deviation, $n \geq 3$, $^{*}P < 0.05$, $^{**}P < 0.01$. (C) Representative images of wound healing assay conducted in OVCA cells (SKOV3 and CaOV3) transfected with pCMV-FLAG-ezrin (FLAG-ezrin) or pCMV-FLAG empty vector (FLAG-vector).

Rho GTPases through interaction with Rho guanine nucleotide exchange factors [GEFs (RhoGEFs)], Rho GTPase-activating proteins (RhoGAPs), and Rho GDP dissociation inhibitors. The small GTPases Rho and Rac regulate the assembly of actin filament and the formation of integrin adhesion complexes to produce stress fibers and lamellipodia, respectively, in mammalian cells[17,18]. We conducted RhoA and Rac active pull down assays to determine the pathogenic pathway of ezrin in epithelial OVCA cells. Using the anti-RhoA antibody, the immunosignal of GTP-RhoA (isolated and pulled down by Rhotekin RBD beads) was much stronger in SKOV3 and CaOV3 cells transfected with FLAG-ezrin expressing plasmids compared with that in the cells transfected with FLAG-vector control plasmids; conversely, GTP-RhoA immunosignals weakened after the downregulation of ezrin in SKOV3 and CaOV3 cells, although no significant difference was observed in RhoA expression in these cell lysates (Figure 5A and 5B). When the anti-Rac1 antibody was used to detect the protein pulled down by human p21 activated kinase 1 protein (PAK) Rac/Cdc42 (p21) binding domain agarose beads and total protein from SKOV3 and CaOV3 cells, the

immunosignal intensity remained unchanged by either an increase or decrease in ezrin expression (Figures 5C and 5D). These results indicate that although ezrin had no effect on small Rho GTPases expression, it activates RhoA.

Ezrin is mainly located in the cytoplasm, and a proportion of it is colocalized with F-actin. The N-terminal FERM domain of ezrin can bind to the cytoplasmic tail of membrane proteins, and its C-terminal domain interacts with F-actin, resulting in actin filament remodeling, cell motility, invasion, and carcinoma metastasis[14]. To obtain visible evidence regarding ezrin in cultured SKOV3 and CaOV3 cells, we performed indirect immunofluorescence staining of ezrin, followed by confocal scanning. Cells were transfected with pCMV-FLAG-ezrin or pCMV-FLAG empty vector for 24 h and then subjected to fluorescence staining, as described in 'Materials and Methods'. Figure 6A shows that cells transfected with pCMV-FLAG empty vector were smooth and rounded, with no membrane ruffling and almost no protrusions or stress fibers. The FLAG was evenly distributed throughout the cell, with little staining in the membrane. By contrast, when the cells were
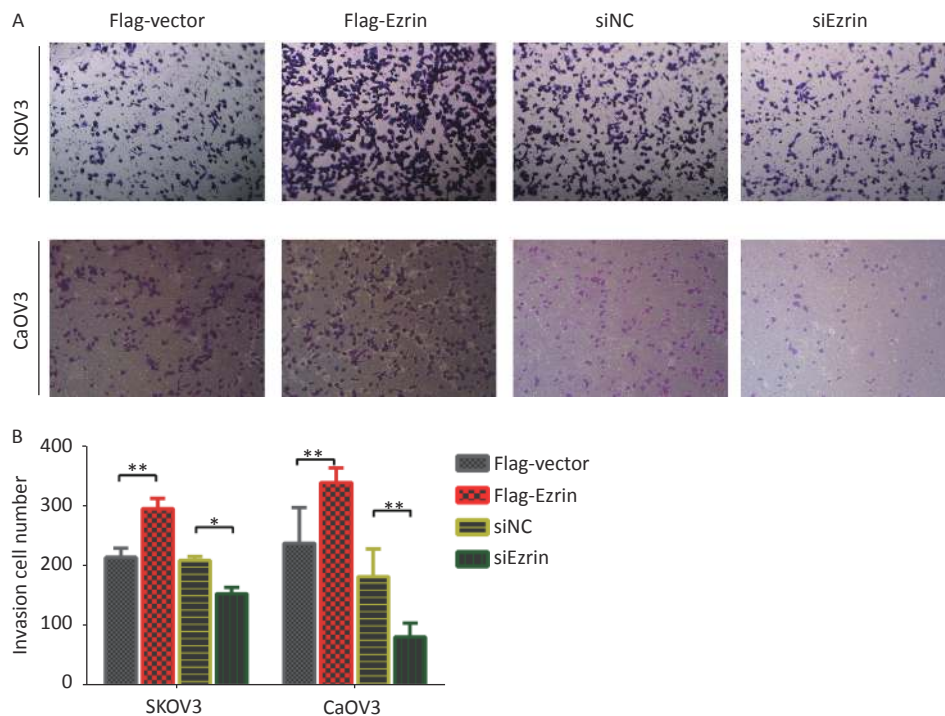

Figure 3. Effects of ezrin on cell invasion in ovarian carcinoma cells. (A) Cell invasion assay and (B) quantification showed invasiveness of OVCA cells (SKOV3 and CaOV3) transfected with pCMV-FLAG-ezrin (FLAG-ezrin), pCMV-FLAG empty vector (FLAG-vector), siNC, siEzrin. Data are presented as mean ± standard deviation, $n \geq 3$, $^{*}P < 0.05$, $^{**}P < 0.01$.

transfected with pCMV-FLAG-ezrin expressing plasmids, cells changed shape. The cell flattened and formed membrane ruffling and protrusions. Thick and bundled filaments, which are similar to actin stress fibers, traversed the cell body. Immunoreactive FLAG-ezrin had moved to and was concentrated in the area of actin stress fibers. However, the effect of ectopic ezrin on stress fiber

reorganization can be abolished by C3 transferase and specific inhibitors of RhoA[19]; however, C3 does not completely eliminate the formation of cell membrane ruffling caused by ectopic ezrin. The same effect was observed in CaOV3 cells (Figure 6B). These results suggest that ezrin is related to the morphological changes in the EMT and actin filament remodeling processes.
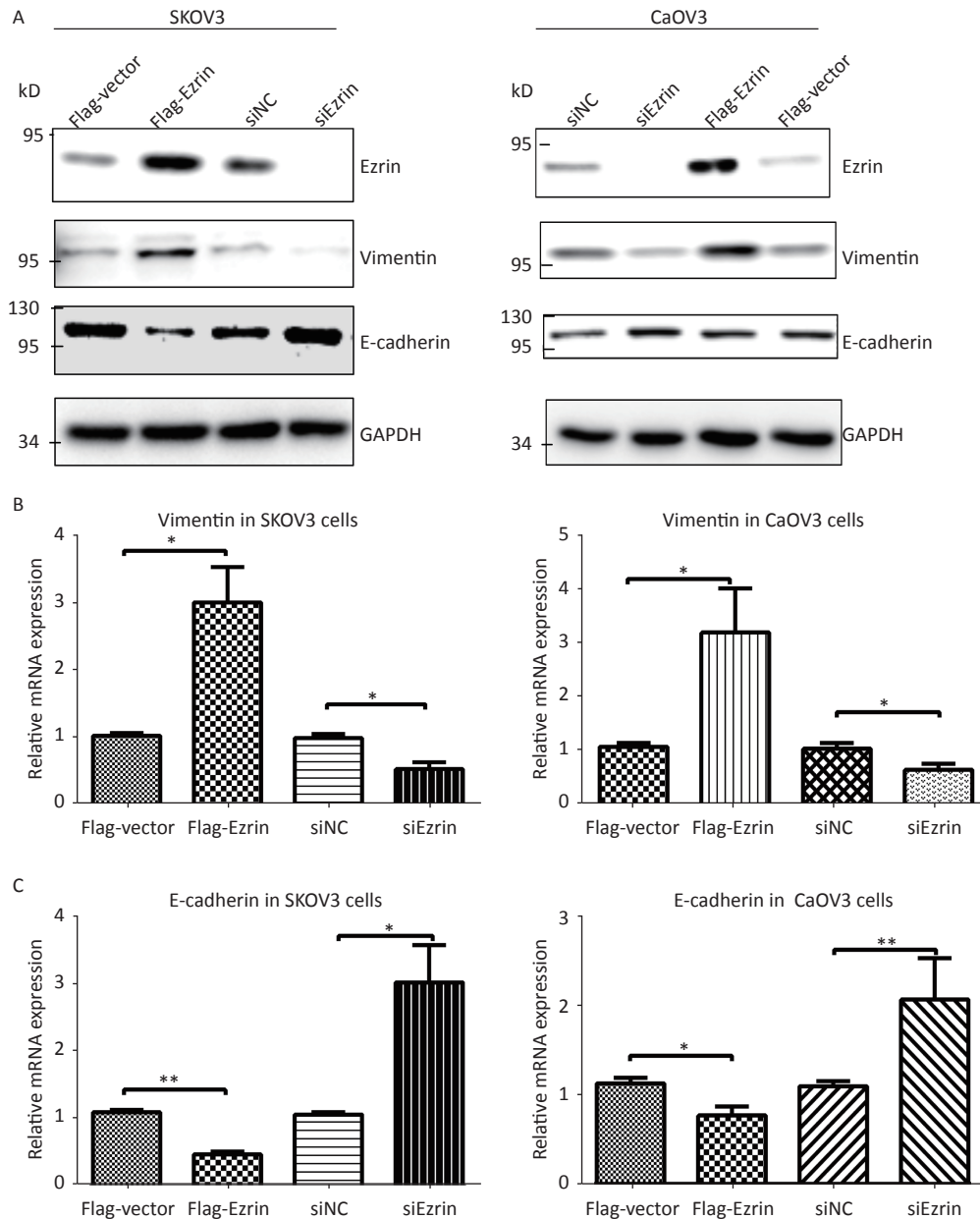

Figure 4. Effects of ezrin on EMT in ovarian carcinoma cells. SKOV3 and CaOV3 cells were transfected with pCMV-FLAG-ezrin (FLAG-ezrin), pCMV-FLAG empty vector (FLAG-vector), siNC, anti-ezrin siRNA for 24 h and then harvested for Western blot analysis and RT-qPCR. (A) Western blot analysis showed the protein level of ezrin and EMT-associated markers (E-cadherin and vimentin). RT-qPCR showed the mRNA level of vimentin (B) and E-cadherin (C) in SKOV3 and CaOV3 cells. $^*P < 0.05$, $^{**}P < 0.01$.

DISCUSSION

OVCA is the most common cause of death in women with gynecological malignancy. However, the therapeutic effectiveness of treatments for OVCA is not ideal at present. Most patients with OVCA die from the advanced stage (metastatic) of the cancer[6-8,20,21]. Similar to other solid cancers, the occurrence of metastasis and invasion is an important contributing factor for OVCA mortality. Therefore, understanding the mechanism underlying the metastasis of OVCA is crucial.
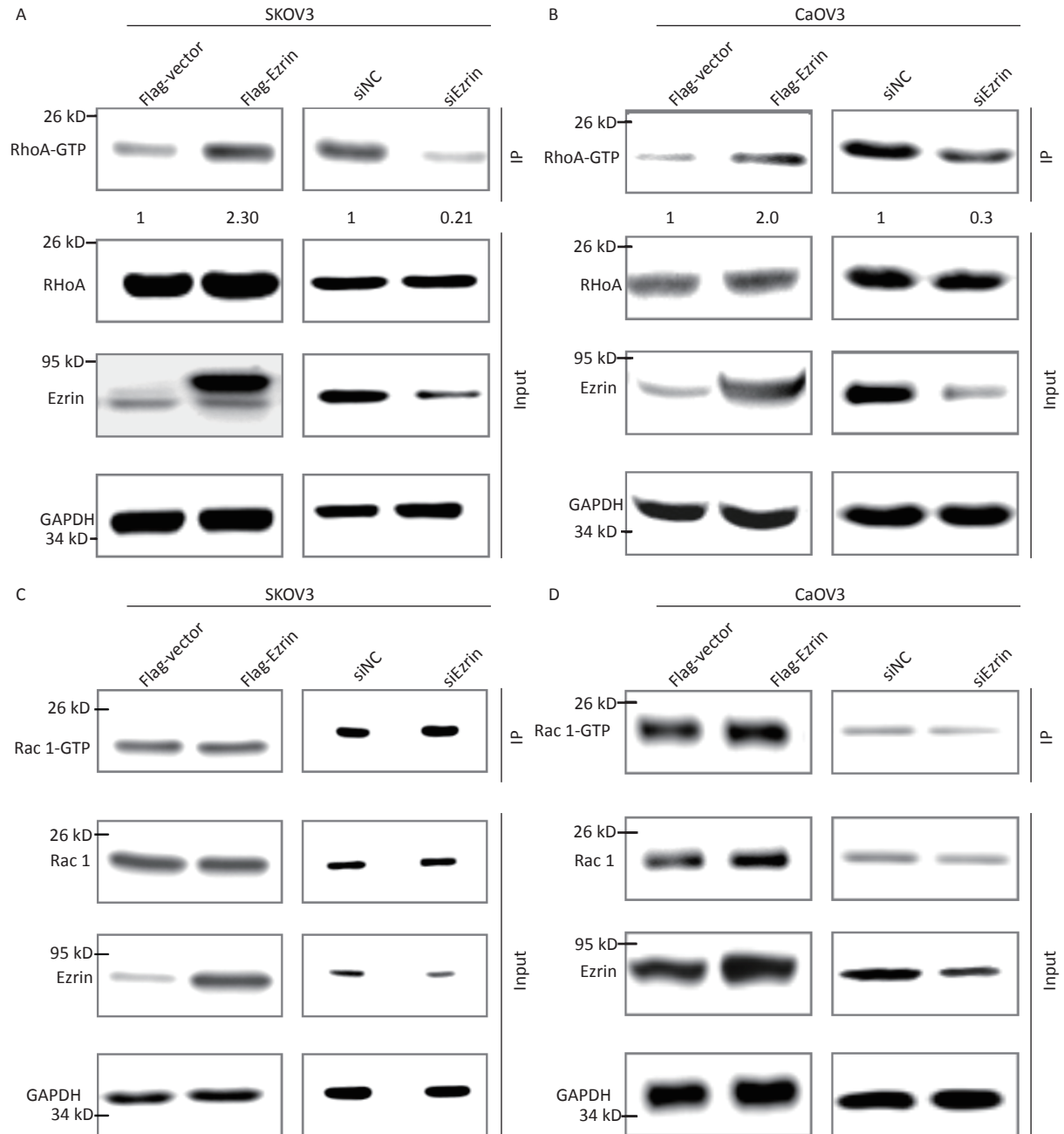

Figure 5. Ezrin regulates RhoA GTPase activity. Analysis of RhoA activation levels after the overexpression or knockdown of ezrin in SKOV3 (A) and CaOV3 cells (B) through the immunoprecipitation of their GTP active forms. The ratio of RhoA-GTP and Rho A is shown below. Analysis of Rac1 activation levels after the overexpression or knockdown of ezrin in SKOV3 (C) and CaOV3 (D) through the immunoprecipitation of their GTP active forms.

Numerous studies have demonstrated that ezrin is relevant to various tumors, including glioblastoma[13], pancreatic cancer[22,23], breast cancer[24-26], cervical cancer[10,27], and osteosarcoma[28]. In many cases, increased ezrin expression is correlated to tumor cell growth, survival, and progression[29-31].
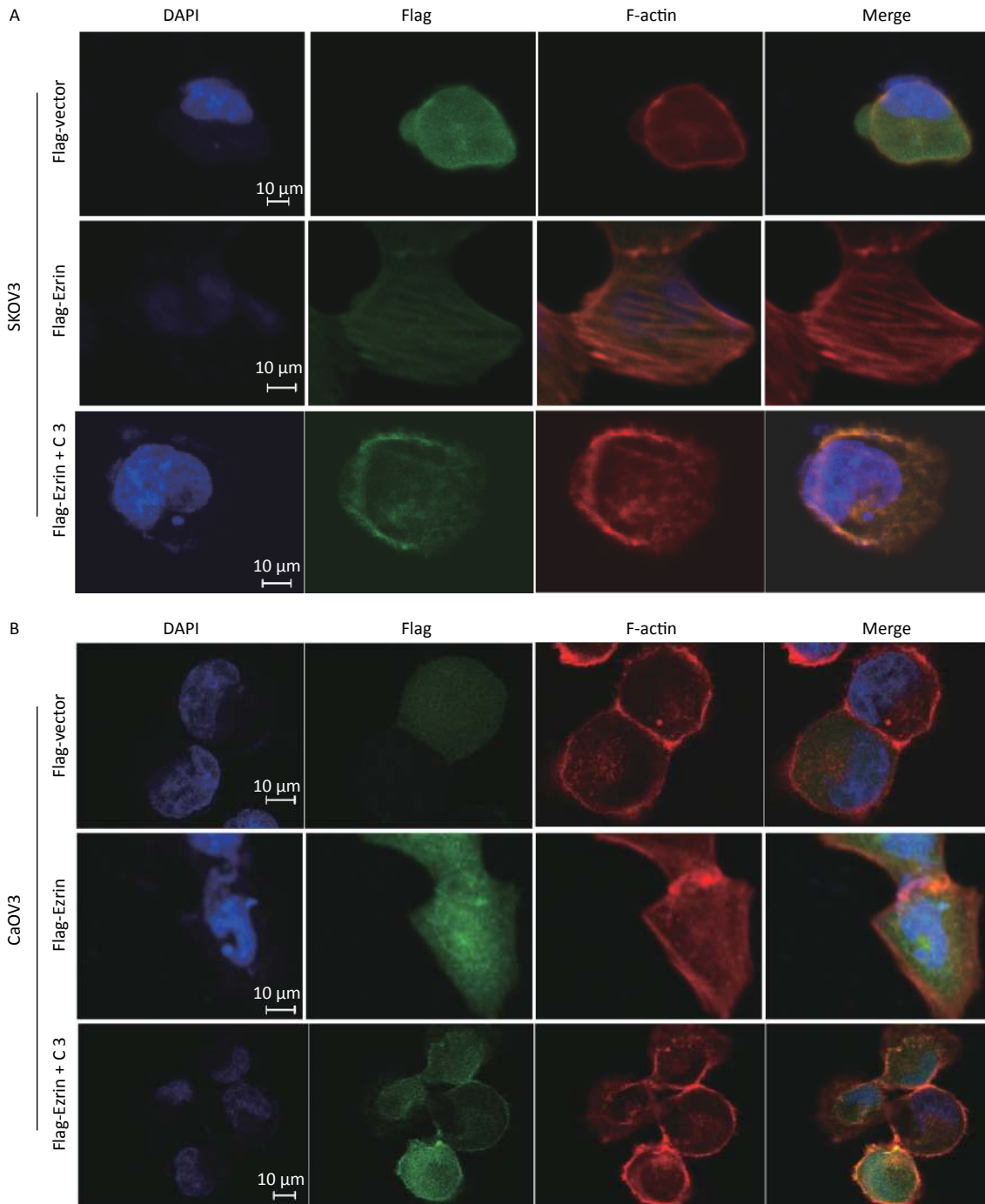

Figure 6. Ezrin stimulates the formation of stress fibers. (A) SKOV3 cells and (B) CaOV3 cells were transfected with either pCMV-FLAG-ezrin (FLAG-ezrin) or pCMV-FLAG empty vector (FLAG-vector) prior to being treated with or without C3 transferase (2 ng/mL). FLAG was detected as described in the Materials and Methods Section (green). F-actin was visualized using Alexa Fluor 568-conjugated phalloidin. Bar: 10 μm.

However, the role of ezrin in the progression of OVCA is controversial in the literature. In a study consisting of 440 ovarian serous adenocarcinomas patients, Moilanen et al.[32] showed that patients with negative or low ezrin expression had a significantly shorter time to progression and shorter survival time than those whose tumors had moderate or high Ezrin expression. Juanni et al.[33] reported that the promotion of HO-8910 OVCA cell invasion by VEGF is due to the downregulation of ezrin caused by miR-205 upregulation. However, Kobel et al.[34] reported that ezrin may be necessary for tumor cell invasion, and lacking ezrin may predict an improved prognosis of ovarian carcinomas. This finding is in accordance with our data. In this study, our results demonstrated that the upregulated expression of ezrin significantly promoted cell growth, EMT, metastasis, and invasiveness in the OVCA cell lines SKOV3 and CaOV3. By contrast, the knockdown of endogenous ezrin prevented ovarian carcinoma cell growth, EMT, metastasis, and invasiveness (Figures 1–4 and Supplementary Figure S1). Our observations revealed that ezrin functions as a tumor promoter in OVCA cells. Combining our results with other reports, we speculated that the effects mediated by ezrin are likely specific to the histological subtypes of ovarian carcinoma or cellular environment.

A growing number of research suggests that during the progression of malignant tumor, the cytoskeleton is strongly altered[21,35-38]. Yin et al.[39] reported that ezrin modulates the RhoA/ROCK and cAMP/PKA signaling pathways, which are key cellular processes associated with asthma. Quang et al.[40] reported that cytoskeletal linker protein ezrin plays an essential role in the transformation of NIH 3T3 fibroblasts by the small G protein RhoA and its GEFs. Francesca et al.[41] examined differential protein expression in cytotoxic gold compound Auoxo6-treated A2780 human ovarian carcinoma cells and found eight altered proteins, of which ezrin is increased. They speculated that the increase in Auoxo6-induced ezrin expression may be considered an initial sign of apoptosis because the apoptotic process involves several rearrangements of the cytoskeleton and cell morphology. In this study, we reported that ezrin activates GTP-RhoA but not Rac1 and induces the formation of robust stress fibers in SKOV3 and CaOV3 cells; these results are consistent with other studies that elevated RhoA/Rho kinase signaling promoting tumor development and metastasis[42,43]. The small GTPase RhoA, plays important roles in the organization of the actin cytoskeleton and is involved in a wide range of fundamental cellular functions, such as contraction, adhesion, migration, proliferation, and apoptosis[16]. Stress fiber formation and membrane ruffling have been ascribed to the activation of RhA or Rac[19,35,44,45]. Our results showed that ezrin overexpression provokes a complex and dramatic reorganization of the actin cytoskeleton and established the physiological role of ezrin-RhoA in cytoskeletal regulation. As shown in Figure 6, membrane ruffles responding to ezrin overexpression were observed in SKOV3 and CaOV3 cells treated with or without C3 transferase. This observation suggests that RhoA is not required for membrane rufflings caused by ezrin overexpression. Moreover, we found that ezrin overexpression does not affect the expression and activity of Rac1 (Figure 5); thus, we speculated that this event was not Rac1-dependent. The regulatory relationship between ezrin and RhoA is complex. Some reports have shown that RhoA can regulate the phosphorylation of ezrin and regulate its activity[46-48], whereas others reported that ezrin can interact with key receptors and adaptors to promote RhoA activation[49-52]; these findings are consistent with the results of the present study. However, many detailed mechanisms must be elucidated. These mechanisms include the relation between RhoA GTPases and ezrin in the activation of stress fiber and membrane ruffle formation and the key players and downstream effectors (ROCK or mDia1) in RhoA signaling that modulate the actin cytoskeleton in response to the down- or upregulation of ezrin; these topics will be explored in our next research[45].

CONCLUSION

Ezrin plays an important role in regulating the growth, metastasis, and invasion of OVCA cells. In the future, ezrin can be used as a new biological marker of OVCA, and the expression level of ezrin can be detected for the early diagnosis of tumors as a marker of tumor metastasis, a therapeutic target, and a standard for the evaluation of prognosis.

COMPETING INTERESTS

The authors declare that there is no competing interest.

AUTHORS' CONTRIBUTIONS

LI Mo Juan and HUANG Hao designed the study and drafted the manuscript. LI Mo Juan, XIONG Dan,

and WEN Zhong Yong carried out the experimental work and analyzed the data. WEN Zhong Yong and HUANG Hao participated in the design of the study and critically reviewed the manuscript and provided intellectual input. All authors read and approved the final version of manuscript.

REFERENCES

1. Dood RL, Zhao Y, Armbruster SD, et al. Defining survivorship trajectories across patients with solid tumors: an evidence-based approach. JAMA Oncol, 2018; 4, 1519–26.

2. Disis ML, Taylor MH, Kelly K, et al. Efficacy and safety of avelumab for patients with recurrent or refractory ovarian sancer: phase 1b results from the JAVELIN solid tumor trial. JAMA Oncol, 2019; 5, 393–401.

3. Pfisterer J, Plante M, Vergote I, et al. Gemcitabine plus carboplatin compared with carboplatin in patients with platinum-sensitive recurrent ovarian cancer: an intergroup trial of the AGO-OVAR, the NCIC CTG, and the EORTC GCG. J Clin Oncol , 2006; 24, 4699–707.

4. Hennessy BT, Coleman RL, Markman M. Ovarian cancer. Lancet (London, England), 2009; 374, 1371–82.

5. Papa A, Caruso D, Strudel M, et al. Update on Poly-ADP-ribose polymerase inhibition for ovarian cancer treatment. J Translat Med, 2016; 14, 267.

6. Coleman RL, Spirtos NM, Enserro D, et al. Secondary surgical cytoreduction for recurrent ovarian cancer. N Engl J Med, 2019; 381, 1929–39.

7. Lheureux S, Gourley C, Vergote I, et al. Epithelial ovarian cancer. Lancet, 2019; 393, 1240–53.

8. Nicosia SV, Bai W, Cheng JQ, et al. Oncogenic pathways implicated in ovarian epithelial cancer. Hematol Oncol Clin North Am, 2003; 17, 927–43.

9. Liu X, Yang T, Suzuki K, et al. Moesin and myosin phosphatase confine neutrophil orientation in a chemotactic gradient. J Exper Med, 2015; 212, 267–80.

10. Zacapala-Gómez AE, Navarro-Tito N, Alarcón-Romero LDC, et al. Ezrin and E-cadherin expression profile in cervical cytology: a prognostic marker for tumor progression in cervical cancer. BMC Cancer, 2018; 18, 349.

11. Kong J, Li Y, Liu S, et al. High expression of ezrin predicts poor prognosis in uterine cervical cancer. BMC Cancer, 2013; 13, 520.

12. Petrilli AM, Fernández-Valle C. Role of Merlin/NF2 inactivation in tumor biology. Oncogene, 2016; 35, 537–48.

13. Morales FC, Molina JR, Hayashi Y, et al. Overexpression of ezrin inactivates NF2 tumor suppressor in glioblastoma. Neuro Oncol, 2010; 12, 528–39.

14. Chen Z, Fadiel A, Feng Y, et al. Ovarian epithelial carcinoma tyrosine phosphorylation, cell proliferation, and ezrin translocation are stimulated by interleukin 1alpha and epidermal growth factor. Cancer, 2001; 92, 3068–75.

15. Song J, Fadiel A, Edusa V, et al. Estradiol-induced ezrin overexpression in ovarian cancer: a new signaling domain for estrogen. Cancer letters, 2005; 220, 57–65.

16. Tang J, Liu C, Xu B, et al. ARHGEF10L contributes to liver tumorigenesis through RhoA-ROCK1 signaling and the epithelial-mesenchymal transition. Exp Cell Res, 2019; 374, 46–68.

17. Mackay DJ, Esch F, Furthmayr H, et al. Rho- and rac-dependent assembly of focal adhesion complexes and actin filaments in permeabilized fibroblasts: an essential role for ezrin/ radixin/moesin proteins. J Cell Biol, 1997; 138, 927–38.

18. Nethe M, Hordijk PL. The role of ubiquitylation and degradation in RhoGTPase signalling. J Cell Sci, 2010; 123, 4011–8.

19. Ory S, Destaing O, Jurdic P. Microtubule dynamics differentially regulates Rho and Rac activity and triggers Rho-independent stress fiber formation in macrophage polykaryons. Eur J Cell Biol, 2002; 81, 351–62.

20. Davis BW, Goldhirsch A, Locher GW, et al. Pathologic data of prognostic significance for remission induction in advanced ovarian carcinoma. J Cancer Res Clin Oncol, 1984; 107, 106–10.

21. Schiewek J, Schumacher U, Lange T, et al. Clinical relevance of cytoskeleton associated proteins for ovarian cancer. J Cancer Res Clin Oncol, 2018; 144, 2195–205.

22. Quan C, Sun J, Lin Z, et al. Ezrin promotes pancreatic cancer cell proliferation and invasion through activating the Akt/mTOR pathway and inducing YAP translocation. Cancer Manag Res, 2019; 11, 6553–66.

23. Penchev VR, Chang YT, Begum A, et al. Ezrin promotes stem cell properties in pancreatic ductal adenocarcinoma. Mol Cancer Res, 2019; 17, 929–36.

24. Li N, Kong J, Lin Z, et al. Ezrin promotes breast cancer progression by modulating AKT signals. Br J Cancer, 2019; 120, 703–13.

25. Ghaffari A, Hoskin V, Turashvili G, et al. Intravital imaging reveals systemic ezrin inhibition impedes cancer cell migration and lymph node metastasis in breast cancer. Breast Cancer Res, 2019; 21, 12.

26. Fröse J, Chen MB, Hebron KE, et al. Epithelial-mesenchymal transition induces podocalyxin to promote extravasation via Ezrin signaling. Cell Rep, 2018; 24, 962–72.

27. Fadiel A, Choi SD, Park B, et al. Expression of Ezrin and estrogen receptors during cervical carcinogenesis. Reprod Sci, 2017; 24, 706–12.

28. Yao Q, Pei Y, Zhang X, et al. microRNA-96 acts as a tumor suppressor gene in human osteosarcoma via target regulation of EZRIN. Life Sci, 2018; 203, 1–11.

29. Zhou J, Feng Y, Tao K, et al. The expression and phosphorylation of ezrin and merlin in human pancreatic cancer. Int J Oncol, 2014; 44, 2059–67.

30. Palou J, Algaba F, Vera I, et al. Protein expression patterns of ezrin are predictors of progression in T1G3 bladder tumours treated with nonmaintenance bacillus Calmette-Guérin. Eur Urol, 2009; 56, 829–36.

31. Tynninen O, Carpén O, Jääskeläinen J, et al. Ezrin expression in tissue microarray of primary and recurrent gliomas. Neuropathol Appl Neurobiol, 2004; 30, 472–7.

32. Moilanen J, Lassus H, Leminen A, et al. Ezrin immunoreactivity in relation to survival in serous ovarian carcinoma patients. Gynecol Oncol, 2003; 90, 273–81.

33. Li J, Li L, Li Z, et al. The role of miR-205 in the VEGF-mediated promotion of human ovarian cancer cell invasion. Gynecol Oncol, 2015; 137, 125–33.

34. Köbel M, Gradhand E, Zeng K, et al. Ezrin promotes ovarian carcinoma cell invasion and its retained expression predicts poor prognosis in ovarian carcinoma. Int J Gynecol Pathol, 2006; 25, 121–30.

35. Ruiz-Loredo AY, López E, López-Colomé AM. Thrombin promotes actin stress fiber formation in RPE through Rho/ROCK-mediated MLC phosphorylation. J Cell Physiol, 2011; 226, 414–23.

36. Fife CM, McCarroll JA, Kavallaris M. Movers and shakers: cell

cytoskeleton in cancer metastasis. Br J Pharmacol, 2014; 171, 5507–23.

37. Araki K, Ebata T, Guo AK, et al. p53 regulates cytoskeleton remodeling to suppress tumor progression. Cell Mol Life Sci, 2015; 72, 4077–94.

38. Hu L, Huang Z, Wu Z, et al. Mammalian plakins, giant cytolinkers: versatile biological functions and roles in cancer. Int J Mol Sci, 2018; 19.

39. Yin LM, Duan TT, Ulloa L, et al. Ezrin orchestrates signal transduction in airway cells. Rev Physiol Biochem Pharmacol, 2018; 174.

40. Tran Quang C, Gautreau A, Arpin M, et al. Ezrin function is required for ROCK-mediated fibroblast transformation by the Net and Dbl oncogenes. EMBO J, 2000; 19, 4565–76.

41. Magherini F, Modesti A, Bini L, et al. Exploring the biochemical mechanisms of cytotoxic gold compounds: a proteomic study. J Biol Inorg Chem, 2010; 15, 573–82.

42. Gur S, Kadowitz PJ, Hellstrom WJG. RhoA/Rho-kinase as a therapeutic target for the male urogenital tract. J Sex Med, 2011; 8, 675–87.

43. Assao A, Nonogaki S, Lauris JRP, et al. Podoplanin, ezrin, and Rho-A proteins may have joint participation in tumor invasion of lip cancer. Clin Oral Investig, 2017; 21, 1647–57.

44. Okamoto H, Takuwa N, Yokomizo T, et al. Inhibitory regulation of Rac activation, membrane ruffling, and cell migration by the G protein-coupled sphingosine-1-phosphate receptor EDG5 but not EDG1 or EDG3. Mol Cell Biol, 2000; 20, 9247–61.

45. Tsuji T, Ishizaki T, Okamoto M, et al. ROCK and mDia1 antagonize in Rho-dependent Rac activation in Swiss 3T3 fibroblasts. J Cell Biol, 2002; 157, 819–30.

46. Ma L, Liu YP, Zhang XH, et al. Effect of RhoA signaling transduction on expression of Ezrin in breast cancer cell lines. Cancer, 2009; 28, 108–11.

47. Song Y, Wong C, Chang DD. Overexpression of wild-type RhoA produces growth arrest by disrupting actin cytoskeleton and microtubules. J Cell Biochem, 2000; 80, 229–40.

48. Yonemura S, Matsui T, Tsukita S, et al. Rho-dependent and -independent activation mechanisms of ezrin/radixin/moesin proteins: an essential role for polyphosphoinositides in vivo. J Cell Sci, 2002; 115, 2569–80.

49. Takahashi K, Sasaki T, Mammoto A, et al. Direct interaction of the Rho GDP dissociation inhibitor with ezrin/radixin/moesin initiates the activation of the Rho small G protein. J Biol Chem, 1997; 272, 23371–5.

50. Schmieder S, Nagai M, Orlando RA, et al. Podocalyxin activates RhoA and induces actin reorganization through NHERF1 and Ezrin in MDCK cells. J Am Soc Nephrol, 2004; 15, 2289–98.

51. Menager C, Vassy J, Doliger C, et al. Subcellular localization of RhoA and ezrin at membrane ruffles of human endothelial cells: differential role of collagen and fibronectin. Exp Cell Res, 1999; 249, 221–30.

52. Jiang QY, Xia JM, Ding HG, et al. RNAi-mediated blocking of ezrin reduces migration of ectopic endometrial cells in endometriosis. Mol Hum Reprod, 2012; 18, 435–41.
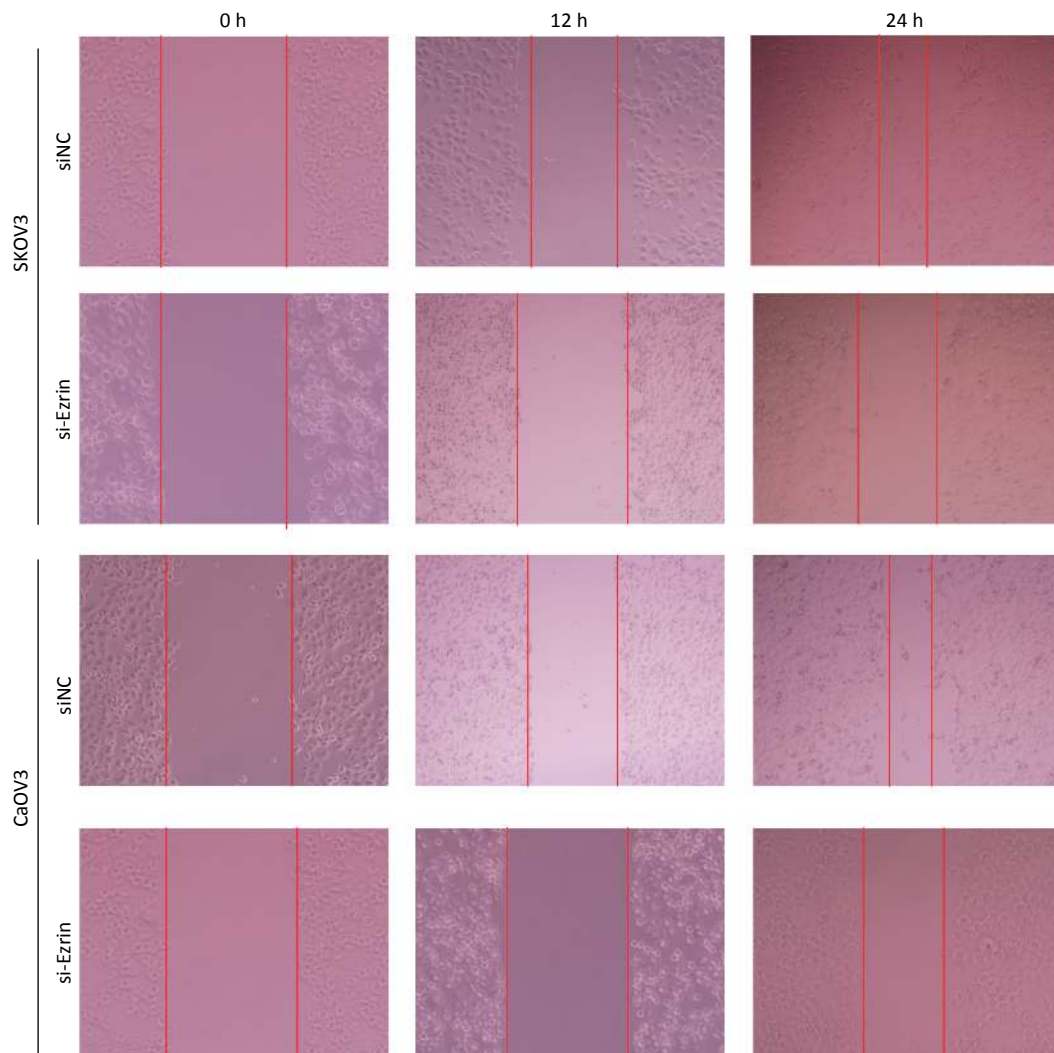
Supplementary Figure S1. Representative images of wound healing assay carried out in ovarian cancer cells (SKOV3 and CaOV3) transfected with siNC, si-Ezrin.